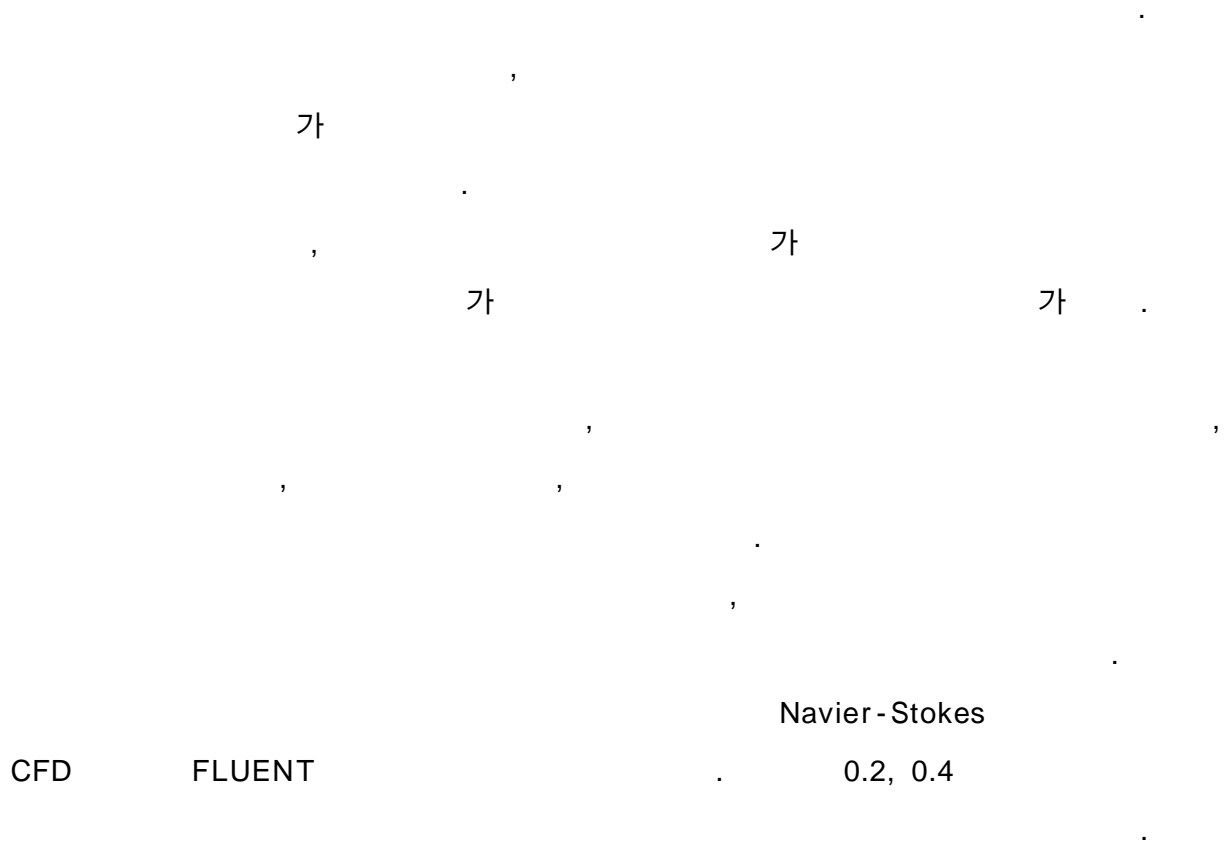


A Numerical Investigation of Aerodynamic Characteristics of
Asymmetric Flowfields on Slender Bodies
at the High Angle of Attack



Keywords: , , Navier-Stokes CFD

1.

가

가

가

가

25

가

가

가

. Euler

가

CFD

2.

[1]

가 Missile

Sideslip

가

($\alpha = 5^\circ$) Attached

Flow 가 Cross Flow가

[3] $5^\circ < \alpha < 25^\circ$ 가

25° 60°

($25^\circ < \alpha < 60^\circ$) Karman

Vortex Street Point Body

Nose Blunt Body Nose가

Nose .[2]

2.1

가

(Laminar Separation, Turbulent

Separation.)

가 가

Figs. 1,2 가

가

가

[2,11]

50

가

.[Fig. 1,2]

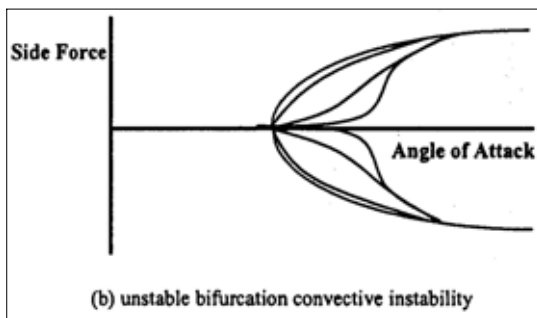


Fig. 1.

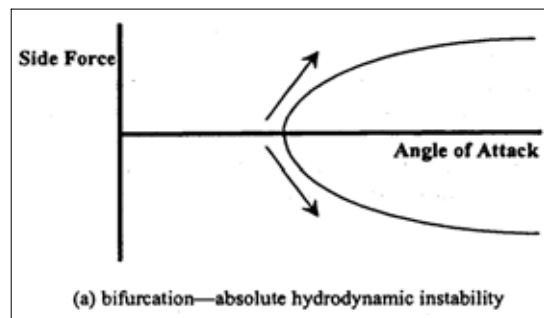


Fig. 2.

2.2

가

.[2]

$$C_Y = f(\alpha, M, Re_D)$$

Nose
 .[2]
 M>0.8

Fuselage
 M=0.5
 Zero

가 가

가 Leeward

$0.5 \sim 1 \times 10^6$

$0.5 \sim 1 \times 10^6$

Leeward

$\phi > 140^\circ$

가

$Re_D \approx 0.45 \times 10^6$

3.

가

가

3.1

Navier - Stokes

$$\frac{\partial Q}{\partial t} + \frac{\partial E}{\partial x} + \frac{\partial F}{\partial y} + \frac{\partial G}{\partial z} = \frac{1}{Re} \left(\frac{\partial E_\nu}{\partial x} + \frac{\partial F_\nu}{\partial y} + \frac{\partial G_\nu}{\partial z} \right)$$

Law-of-the-Wall

$$\frac{u_p \rho^*}{\tau_w / \rho} = \frac{1}{k} \ln \left(E \frac{\rho^* y_p}{\mu} \right) - \Delta B$$

ΔB

$$\Delta B = \frac{1}{k} \ln \left[\frac{K_s^+ - 2.25}{87.75} + C_{K_s} K_s^+ \right] \times \sin 0.4258 (\ln K_s^+ - 0.811)$$

$$K_s^+ = \rho K_s \rho^* / \mu, \quad K_s, \quad C_{K_s}$$

$$K_s = 1 \text{ mm}, \quad C_{K_s} = 0.5$$

0.26

Cell

(FVM),

(Implicit), Roe FDS

2

(Upwind Scheme),

1

K-e

$$C_\mu = 0.09, \quad C_{\epsilon 1} = 1.44, \quad C_{\epsilon 2} = 1.92, \quad \sigma_k = 1.0, \quad \sigma_\epsilon = 1.3$$

3.2

:

Navier-Stokes

[8,9,10]

, FVS (Flux Vector Splitting), Implicit, Block Tridiagonal

Matrix

Navier-Stokes

가

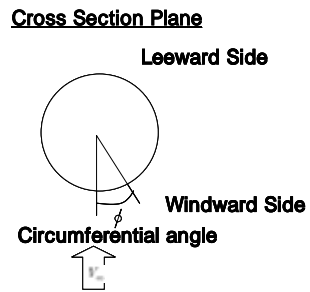
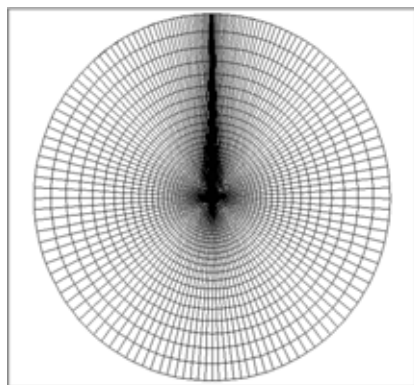


Fig. 3.

Fig. 3

Leeward

Windward

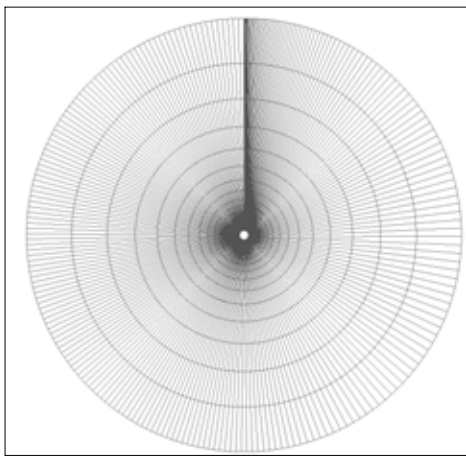


Fig. 4.

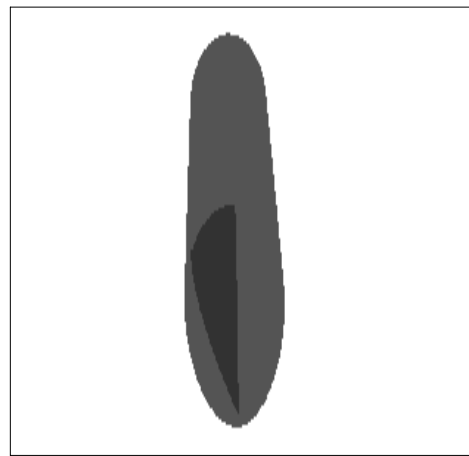


Fig. 5.
 $(180^\circ < \phi < 240^\circ)$

Fig. 4

[9] Fig. 5

Slender Body

$(180^\circ < \phi < 240^\circ)$

가

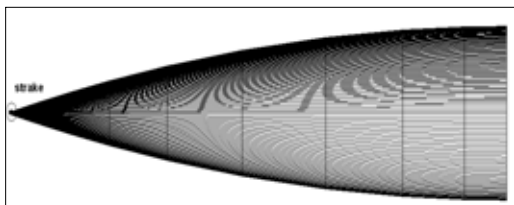


Fig. 6.
(0.035D strake, $\phi=240$)

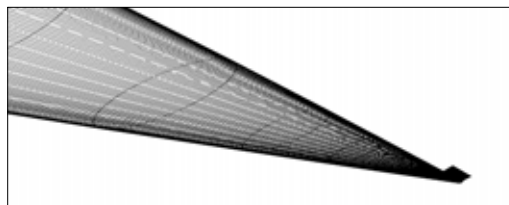


Fig. 7. Strake
(0.035D strake, $\phi=240$)

Fig. 6 Strake 240 1
0.035D [7]
240 Missile
Fig. 7 Fig. 6

Strake

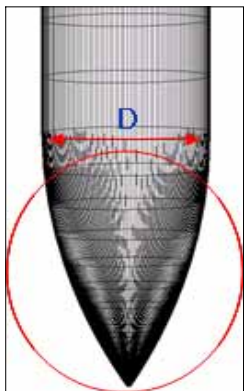


Fig. 8

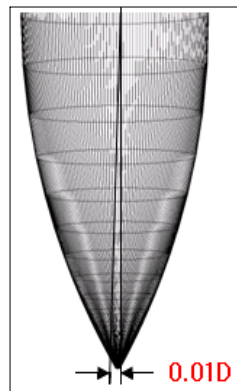


Fig. 9

Fig. 8 Missile

가

. Body 0.01D
 270 . Fig. 9 Fig. 8

Table 1

	sideslip angle 0.5°
	180°<phi<240°
	Roughness height=1.0mm
	0°<phi<180°, 240°<phi<360°
	Roughness height=0.0mm
Strake	0.035D, Phi=240°
	0.01D, Phi=270°

Table 1.

3.3

Missile

Slender Body

. Navier-Stokes

CFD

.[Table 2]

[7,10,11]

	30
	0.2
	3.0E+06

Table 2. CFD

3.3.1

CAD CATIA Gridgen
 Tangent-Ogive Cylinder 1.2m Fig. 10



Fig. 10.

Fig. 11

6 Block 가 , 600,000

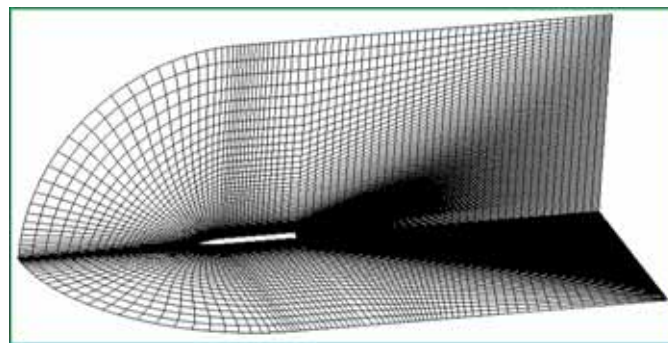


Fig. 11. 3

No Slip
 , Cylinder (0°<phi <180°, 240°<phi<360°)
 (180°<phi< 240°)

1mm

3.3.2

[Fig. 12]

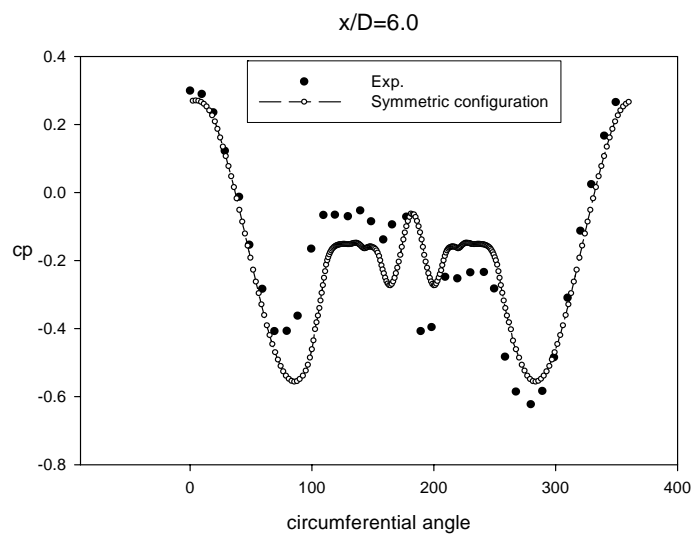


Fig. 12.

$(M_\infty=0.2, \alpha=30^\circ, Re_D=3.0 \times 10^6)$

Fig. 13 $x/D=6.0$

$180^\circ < \phi < 240^\circ$

가

가

$(240^\circ < \phi < 250^\circ)$

[7]

.[7]

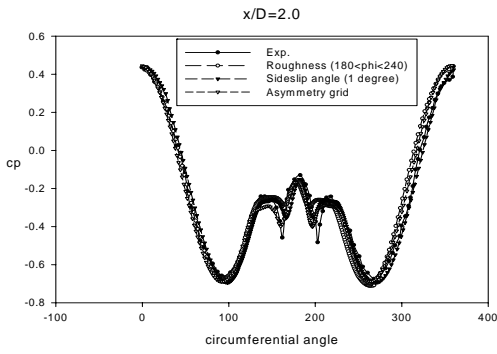


Fig. 15.

$(M_\infty=0.2, \alpha=30^\circ, Re_D=3.0 \times 10^6)$

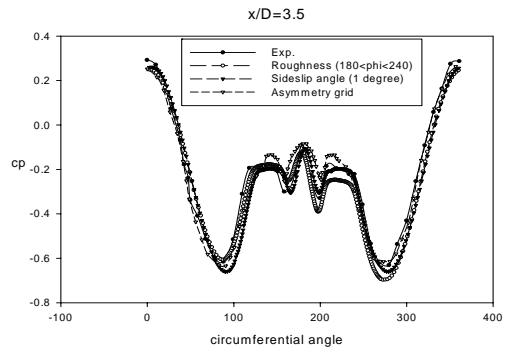


Fig. 16.

$(M_\infty=0.2, \alpha=30^\circ, Re_D=3.0 \times 10^6)$

Fig. 17 x/D=5.0

가

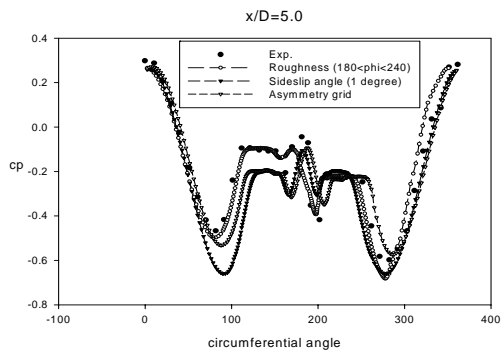


Fig. 17.

$(M_\infty=0.2, \alpha=30^\circ, Re_D=3.0 \times 10^6)$

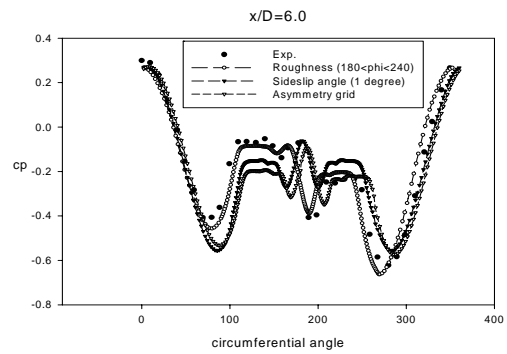


Fig. 18.

$(M_\infty=0.2, \alpha=30^\circ, Re_D=3.0 \times 10^6)$

가

가

.[2]

.[13]

Fig. 18 $x/D=6.0$

가

가 가

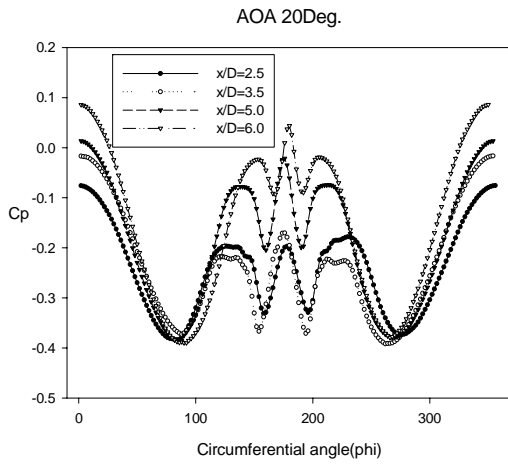


Fig. 19.

$(M_\infty=0.4, \alpha=20^\circ, Re_D=6.0 \times 10^6)$.

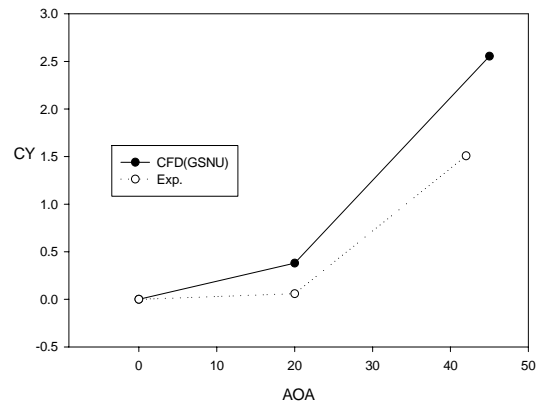


Fig. 20.

$(CFD: M_\infty=0.4, Re_D=6.0 \times 10^6)$
 $Exp: M=0.25, Re_D=30,000)$

Fig. 19

가

. Fig. 19

20

, Fig. 20

20

.[2,13]

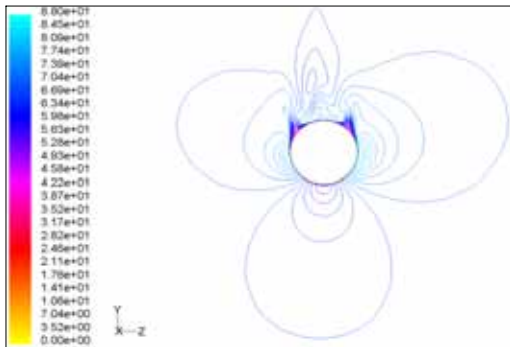


Fig. 21.
 $(M_\infty=0.2, \alpha=30^\circ, Re_D=3.0 \times 10^6)$

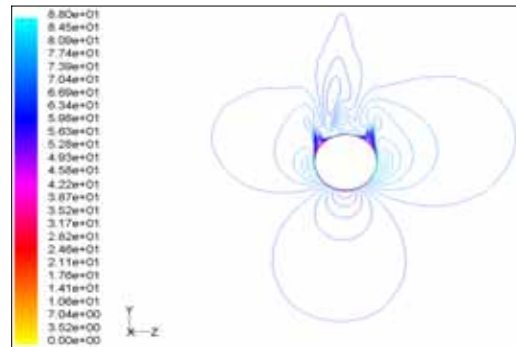


Fig. 22.
 $(M_\infty=0.2, \alpha=30^\circ, Re_D=3.0 \times 10^6)$

Figs. 21, 22 $x/D=5.0$ $x/D=6.0$

가

가

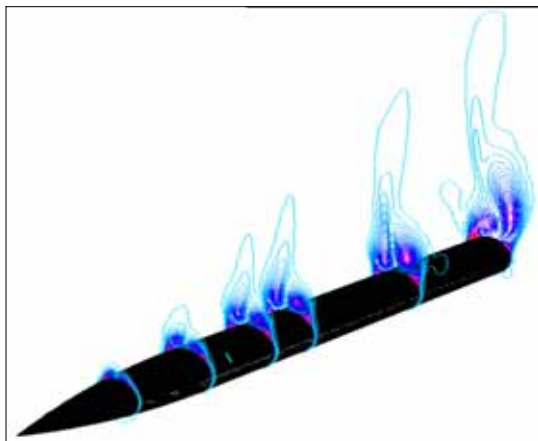


Fig. 23.

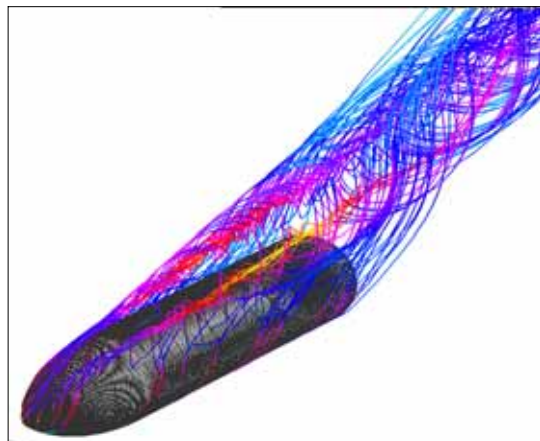


Fig. 24. Slender body

Fig. 23 Slender Body

가 가 Body
가 가
[2]

Fig. 24 Slender Body

가 가
[10] 가

3.4

3.4.1 CFD

Fig. 25 Slender Body 가

[13] Body

RPM

Slender Body

Fig. 26

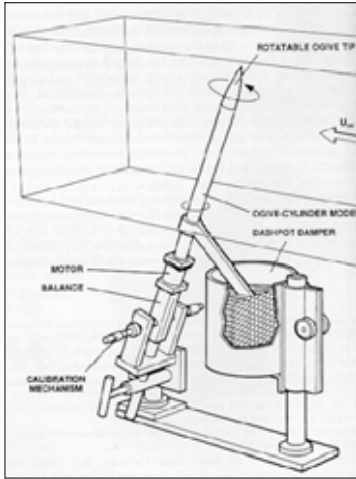


Fig. 25.



Fig. 26. CFD

Table 3

CFD

가

	0.25	30,000
CFD	0.4	600,000

Table 3.

CFD

3.4.2

Fig. 27 20

20
[13]

가

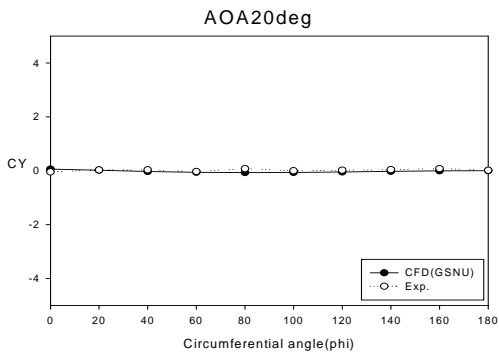


Fig. 27.
($M_\infty=0.4$, $\alpha=20^\circ$, $Re_D=6.0 \times 10^5$)

CFD

Fig. 28 35

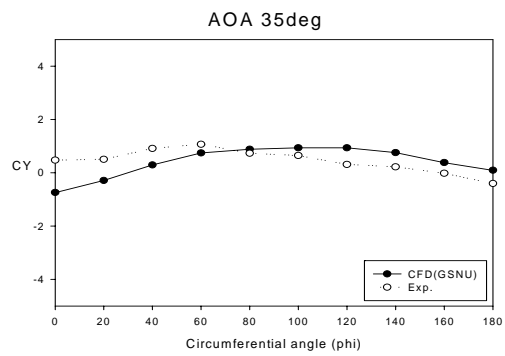


Fig. 28.
($M_\infty=0.4$, $\alpha=35^\circ$, $Re_D=6.0 \times 10^5$)

Fig. 29 42

0 40

Navier-Stokes

Fig. 2

가

Fig. 30 50

160 180

50

CFD

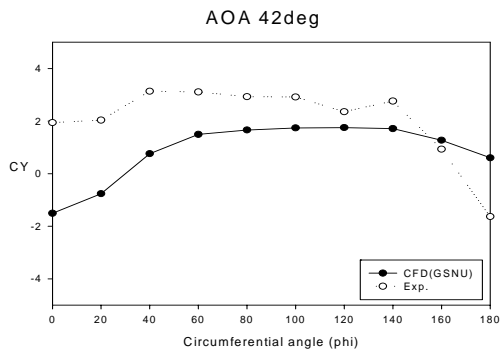


Fig. 29.

$(M_\infty=0.4, \alpha=42^\circ, Re_D=6.0 \times 10^6)$

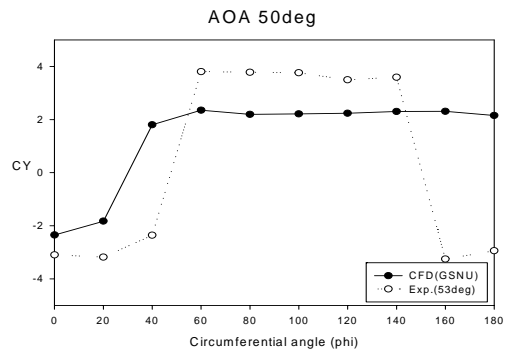


Fig. 30.

$(M_\infty=0.4, \alpha=50^\circ, Re_D=6.0 \times 10^6)$

가

80

가

가

3.5

600,000 , Block 6

3.5.1

Tangent-Ogive

Fig. 10

- Secant-Ogive

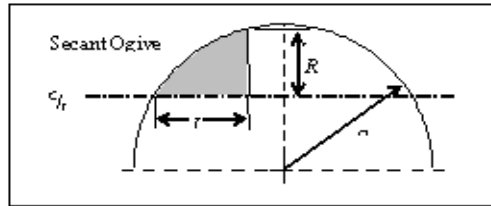


Fig. 31. Secant ogive drawing

$$\rho = \frac{R^2 + L^2}{2R} \quad \alpha = \tan^{-1}\left(\frac{R}{L}\right) - \cos^{-1}\left(\frac{\sqrt{L^2 + R^2}}{2\rho}\right)$$

x

y

$$y = \sqrt{\rho^2(x - \rho \cos \alpha)^2 + \rho \sin \alpha}$$

- Power Series

Power Series

n=0.75 n=0.5

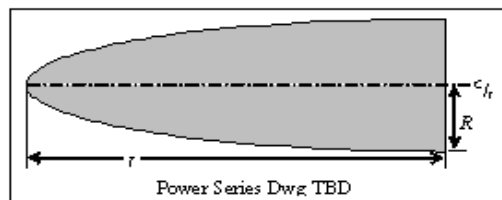


Fig. 32. Power series drawing

For $0 \leq n \leq 1$, $y = R \left(\frac{x}{L} \right)^n$

: $n = 1$ for a **CONE**

$n = .75$ for a **¾ POWER**

$n = .5$ for a **½ POWER (PARABOLA)**

$n = 0$ for a **CYLINDER**

- Haack series

Haack Series

$C=1/3$ $C=0.0$

. $C=0$

Von Karman

Von Karman Ogive

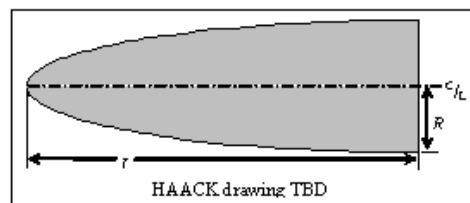


Fig. 33 Haack series drawing

$$\theta = \cos^{-1} \left(1 - \frac{2x}{L} \right) , \quad y = \frac{R \sqrt{\theta - \frac{\sin(2\theta)}{2} + C \sin^3 \theta}}{\sqrt{\pi}}$$

: $C = 1/3$ for **LV-HAACK**

$C = 0$ for **LD-HAACK**

3.5.2

Fig. 34 $x/D=2.0$

$x/D=2.0$

가

가

Fig. 35 $x/D=3.5$

가

Tangent-Ogive

Secant-Ogive

$x/D=3.5$

Secant-Ogive

$x/D=3.5$

(Blunt)

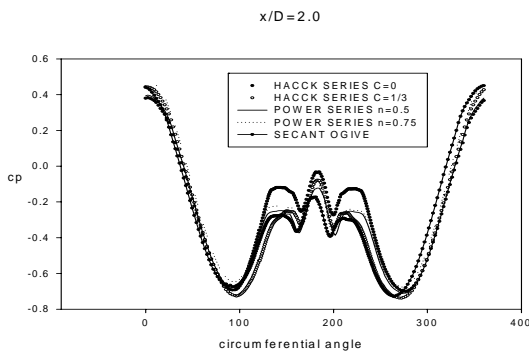


Fig. 34.

$(M_\infty=0.2, \alpha=30^\circ, Re_D=3.0 \times 10^6)$

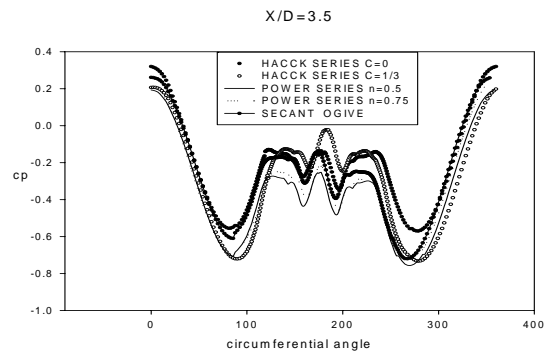


Fig. 35.

$(M_\infty=0.2, \alpha=30^\circ, Re_D=3.0 \times 10^6)$

Fig. 36 $x/D=5.0$

가

Haack Series C=0

Haack Series가 가 Blunt

Fig. 37 $x/D=6.0$ $x/D=5.0$
 가

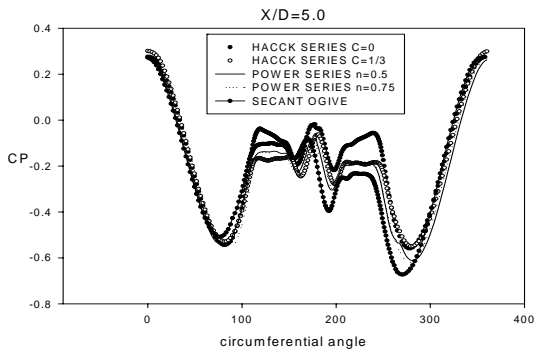


Fig. 36
 $(M_\infty=0.2, \alpha=30^\circ, Re_D=3.0 \times 10^6)$

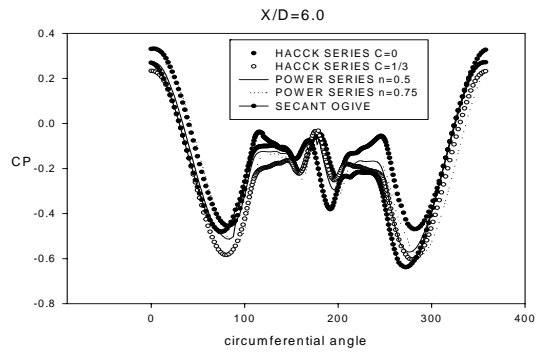


Fig. 37
 $(M_\infty=0.2, \alpha=30^\circ, Re_D=3.0 \times 10^6)$

4.

Tangent Ogive-Cylinder

가

Navier-Stokes

20-50

, 50-65

Blowing, Suction, Strake

Fin

가

가

Navier-Stokes

- [1] Dunne, A. L., Black, S., Schmidt, G. S., and Lewis, T. L., □□VLA Missile Development and High Angle of Attack Behavior, □□ *NTIS N90-17553*, 1990.
- [2] Champigny, P., □□High Angle of Attack Aerodynamics, □□ *AGARD Report 804 (Special Course on Missile Aerodynamics)*, 1994.
- [3] Luo, S. C. et al., □□Flowfield Around Ogive/Elliptic-tip Cylinder at High Angle of Attack, □□ *AIAA Journal*, Vol. 36, No. 10, pp. 1778-1787, 1998.
- [4] Yuan, C. C. and Howard, R. M., □□Effects of Forebody Strakes on Asymmetric Vortices for a Vertically-Launched Missile, □□ *AIAA Paper 91-2864-CP*, 1991.
- [5] Westmoreland, S. and Gebert, G., □□Strake Effectiveness for Controlling Out-of-Plane Loading on Missile Configuration, □□ *AIAA Paper 2000-0386*, 2000.
- [6] Venugopal, S. and Krishnamurthy, M., □□Missile Aerodynamics at High Angle of Attack: A Prediction Code, □□ *AIAA Journal*, Vol. 32, No. 2, p. 263, 1995.
- [7] 김민준, □□ 고각에서의 기체 유동 특성에 대한 연구, □□ *항공우주학회지*, Vol. 22, No. 1, pp. 1-10, 1996.
- [8] Lamont, P. J., □□Pressure Around an Inclined Ogive Cylinder with Laminar, Transitional, or Turbulent Separation, □□ *AIAA Journal*, Vol. 20, No. 11, pp. 1492-1499, 1982.
- [9] Degani, D., □□Effect of Geometrical Disturbance on Vortex Asymmetry, □□ *AIAA Journal*, Vol. 29, No. 4, pp. 560-566, 1991.
- [10] Degani, D. and Schiff, L. B., □□Numerical Simulation of the Effect of Spatial Disturbances on Vortex Asymmetry, □□ *AIAA Paper 89-0340*, 1989.
- [11] Cummings, R. M., Forsythe, J. R., Morton, S. A., and Squires, K. D., □□Computational Challenges in High Angle of Attack Flow Prediction, □□ *Progress in Aerospace Sciences*, Vol. 39, pp. 369-384, 2003.

- [12] Wilcox, D. C., □□ *Turbulence Modeling for CFD*, □□ 2nd ed., DCW Industries, 2002.
- [13] Zilliac, G. G., □□ Asymmetric vortices on a slender body of revolution, □□ *AIAA Journal*, Vol. 29, No. 5, pp. 667-675, 1991.
- [14] Zeiger, M. D., Telionis, D. P., and Vlachos, P. P., □□ Unsteady Separated Flows over Three-Dimensional Slender Bodies, □□ *Progress in Aerospace Sciences*, Vol. 40, pp. 291-320, 2004.
- [15] Lesage, F., Nicolle, J., and Boulianne, M. A., □□ Navier-Stokes Computations of High Angle of Attack Missile Flowfields, □□ *AIAA Paper 2000-4212*, 2000